Yossef, Mostafa; Mousavihashemi, Seyedabolfazl; Kallio, Tanja; Puttonen, Jari

Investigation of Combined Electronic and Ionic Thermoelectric Concrete

Published in:
International RILEM Conference on Synergising Expertise towards Sustainability and Robustness of Cement-based Materials and Concrete Structures. SynerCrete 2023

DOI:
10.1007/978-3-031-33211-1_104

Published: 01/01/2023

Document Version
Peer-reviewed accepted author manuscript, also known as Final accepted manuscript or Post-print

Please cite the original version:
Yossef, M., Mousavihashemi, S., Kallio, T., & Puttonen, J. (2023). Investigation of Combined Electronic and Ionic Thermoelectric Concrete. In *International RILEM Conference on Synergising Expertise towards Sustainability and Robustness of Cement-based Materials and Concrete Structures. SynerCrete 2023* (pp. 1163-1175). (RILEM Bookseries; Vol. 43). Springer. https://doi.org/10.1007/978-3-031-33211-1_104

Investigation of Combined Electronic and Ionic Thermoelectric Concrete

Mostafa Yossef[1][0000-0002-4254-9398], Seyedabolfazl Mousavihashemi[1][0000-0001-9014-1189], Tanja Kallio[1][0000-0001-6671-8582], Jari Puttonen[1][0000-0001-6890-0345]

[1] Aalto University, Espoo Finland
mostafa.yossef@aalto.fi

Abstract. Thermoelectric energy is one of the promising renewable energy technologies. Research has been focused on finding new materials that have higher efficiency. While most research focuses on electronic thermoelectric materials based on solid materials, recent research also started to head towards ionic thermoelectricity utilizing the ionic conductivity of liquids and gels. Recently, more materials with p-types thermoelectric properties have been developed than n-type. More n-type thermoelectric materials are needed to be developed to produce more energy from thermoelectric modules. This paper aims to (1) illustrate the concept of combining electronic and ionic thermoelectric material properties, (2) develop an n-type thermoelectric generator using MnO_2 nanopowders and cement paste which acts as a core of the sample, (3) present a novel way to compensate the strength loss through casting high strength concrete shell around the thermoelectric core. Finally, a parametric study is carried out to investigate the role of KOH, MnO_2, inner core size, and the effect of temperature gradient on ionic conductivity.

Keywords: Thermoelectric concrete, ionic conductivity.

1. Introduction

Clean energy is the future of the next generations. It holds the keys to resourceful, sustainable, and affordable energy. Clean energy can be produced from the sun, wind, or even ambient heat in the surrounding environment. One way to have clean energy is to generate energy from temperature differences between two surfaces, known as thermoelectric generation.

The thermoelectric effect was observed in 1822 by Thomas Seebeck and can be measured through different methods. A common method is to measure the Seebeck coefficient, named after Thomas Seebeck. Early investigation of thermoelectric cement paste was started by Wen and Chung[1], [2], who studied the thermoelectric effect of cement with steel and carbon fibers. The recent development of nanomaterials has confirmed that the thermoelectric effect can be used to generate energy. Adding 1% by cement weight of n-type or p-type carbon nanotubes to cement resulted in a Seebeck

coefficient of -500μV/°C and +20μV/°C, respectively [3]. Others have studied the influence of nanopowders on the thermoelectric effect. Adding 5% Bi_2O_3 by weight gave a coefficient of 100μV/°C [4] versus 34 μV/°C, which was achieved by adding 15% of graphene nanoplatelets (GNP) [5]. A relatively high Seebeck coefficient was recorded when adding 15% of silica fume with 5% of nanopowders such as Fe_2O_3, MnO_2, and ZnO, resulting in Seebeck coefficient of 2500 μV/°C, 3085 μV/°C, and 3300 μV/°C, respectively [6], [7].

The previous literature shows that cement with nanopowders has great potential in electronic thermoelectric applications. However, limited research has reported the ionic thermoelectric performance of cements.

Recent research showed that adding 3% ionic liquid 1-butyl-3-methylimidazolium bromide (ILs [Bmim]Br) to an expanded graphite/carbon fiber reinforced cement composite can achieve 746 μV/°C at 80 °C [8]. However, using ILs [Bmim]Br in building materials may be restricted by its expensiveness. This paper aims to develop 1) an n-type thermoelectric effect using inexpensive materials such as MnO_2, cement paste, and KOH, 2) introduce a concept to produce a combined electronic and ionic thermoelectric effect at the same time, and 3) present a novel way to compensate the strength loss and to limit moisture content loss through casting a shell of ultra-high strength concrete (UHSC) around the thermoelectric core.

2. Experiment

2.1. Sample Fabrication

Different samples are manufactured to investigate the behavior of thermoelectric power and ionic conductivity. First, thermoelectric power is measured for the MnO_2 nanopowder sample. Then, core samples are fabricated of cement paste mixed with manganese dioxide to obtain electronic thermoelectricity, and some samples have KOH, which enhances the ionic thermoelectricity. Next, KOH pellets are dissolved in water and added to the sample to ensure by enhancing ionic conductivity full integration of the salts within the sample.

2.2. MnO2 powder

The thermoelectric performance of the MnO_2 is evaluated using two techniques for validation. The first technique uses the physical property measurement system DynaCool™ for controlled thermoelectric measurements. The second one is an in-house setup discussed in detail in the section 2.4.1. For the first measurement technique, the MnO_2 nanopowder is pressed into a pallet of 8 mm length, 3 mm wide, and 2 mm thick. The pallet is then dried in an oven at 80 degrees before measurement. For the second evaluation, a hole with a diameter of 10 mm is drilled in the middle of a 40x40x40 mm foam cube. First, the foam cube is placed on a 1 mm thick copper sheet acting as a

potential and current collector, then the hole is filled with the powder and compacted manually with a metal bar until the hole is filled. Then, another copper sheet is placed on the powder-filled foam cube.

2.2.1. Samples

Samples are fabricated in two stages. The first stage is the core fabrication, consisting of cement paste with a different mix design, as shown in Table 1. The second stage is casting the outer shell consisting of Ultra-High-Strength Concrete (UHSC). The inner core generates electricity through thermoelectric power. The outer shell acts as a load bearing member and keeps moisture of the inner part stable during testing.

Table 1. Mix design for core samples

Electrolyte samples	cement (gm)	water (ml)	Superplasti-cizer (ml)	MnO_2 (gm)	KOH (gm)
S1-MnO_2-cement	17	14	3.5	40	0
S2-MnO_2-cement-1mol. KOH	17	14	3.5	40	0.80
S3-Cement-1m KOH	57	14	3.5	0	0.80

The inner core components are mixed as shown in Table 1 and cast into a 10 mm x 20 mm and 60 mm long mold as shown in Figure 1. Samples are left overnight to be solid enough to fit inside two foam supports engraved with a notch of 10 mm depth to hold both ends of the sample, as shown in Figure 2. The spacing between the foam is 40 mm, and the sample is placed so that the longer side (20 mm) is in the beam depth direction and the smaller side (10 mm) is placed in the middle of the beam~~'s~~ width to facilitate the casting of the concrete.

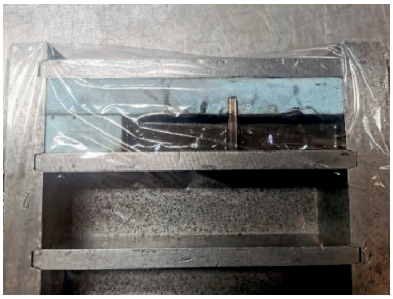

Figure 1. Casting of the first part (MnO_2 and cement paste)

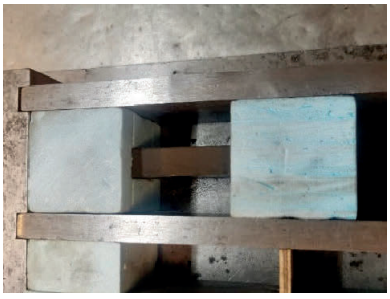

Figure 2. The first part is supported by foam from two sides and placed on the casting mold

Summary of the dimensions of the samples is shown in **Error! Reference source not found.**. The inner core of the group 1 samples has fixed dimensions as these samples undergo thermoelectric and ionic conductivity tests. While the group 2 samples the inner core had different dimensions as these samples are subjected to compressive tests

to study the effect of the core size on strength. The inner core material of the group 2 samples and the sample S1 is same and is shown in Table 1.

Table 2 . Samples dimensions

Group	Sample	Core dimensions			Outer dimensions		
		length (mm)	width (mm)	height (mm)	length (mm)	width (mm)	height (mm)
Group 1	S1-MnO_2-cement	10	20	60	40	40	60
	S2-MnO_2-cement-1mol. KOH						
	S3-Cement-1m KOH						
Group 2	S4-Solid Cube	No core			40	40	40
	S5-Cube with 8mm dia. Core	8mm diameter		40			
	S6-Cube with 10mm dia. Core	10mm diameter		40			
	S7-Cube with 12mm dia. Core	12mm diameter		40			
	S8-Cube with 10*12mm inner core	10	20	40			

Ultra-High Strength Concrete (UHSC) mix design is shown in Table 3. The concrete is cast in the molds surrounding the inner core sample. Samples are left overnight for hardening and then removed from the mold and transferred into a room with 95%±5% relative humidity at 20 °C for curing. After curing, foam is cut and levelled with the surface of the inner core, as shown in Figure 3.

The current and potential collectors shown in Figure 3 consist of 1 mm thick copper plates enclosing a carbon cloth coated with activated carbon powder. The copper plates are connected to the lead wires, while the activated carbon cloths are used for enhanced connection with the inner core. The carbon cloth contains activated carbon particles and is prepared by drop-casting the activated carbon ink onto the carbon cloth. The ink is prepared as follows: 50 mg of the activated carbon is dispersed in 5 ml of NMP by a magnetic stirrer overnight. After that, 0.25 ml of the polyvinylidene fluoride (PVDF)/N-methyl-2-pyrrolidone (NMP) solution (10%) is added to the mix as a binder. Then the suspension is stirred for 4 hours and sonicated for 30 minutes. Finally, the final uniform suspension is drop-casted onto a carbon cloth surface and left to dry at 80 ºC for 30 minutes.

Before testing, 100 ml of water is added to top and bottom of the cores to simulate high relative humidity and further enhance the performance of the samples.

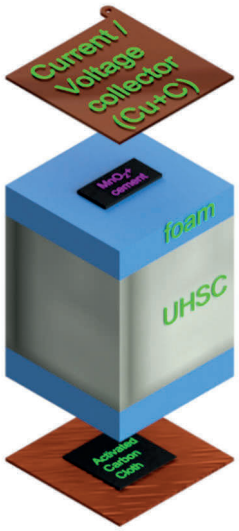

Figure 3. Sample components showing inner core (MnO_2+cement), outer shell (UHSC), and current collectors (Copper plate + Activated Carbon cloth)

Table 3. UHSC mix design

Cement (gm)	500
Silica Fume (gm)	100
Water (ml)	150
SP (ml)	25
Quartz (gm)	188
Sand (gm)	438

2.3. Material Characterization

SEM characterization is used to facilitate the analysis of the nanostructure and morphology of the MnO_2. SEM characterization is done using FEI Quanta FEG 450 equipped with BSE and EDX detector with the voltage set at 15kV. In addition, XRD characterization is carried out using a Rigaku SmartLab X-Ray diffractometer set at high-resolution parallel beam Ge(220)x2/RS. Characterization is done using low X-Ray Fluorescence (XRF) anti-air scatter screen filter to reduce noise.

2.4. Evaluation Setup

2.4.1. Thermoelectric measurements

Copper plates are connected to lead wires to measure the potential difference. For temperature measurements, two thermocouples type K are placed at the top and bottom of the sample between the foam and potential/current collector and connected to a data acquisition system (QuantumX MX840, HBM, Germany) which also measures the potential difference. Peltier module (Laird Thermal Systems, CP14, 127) is placed above the upper current collector to heat the sample, while a heat sink is located underneath the lower face to keep a constant cooling temperature. Testing is carried out at room temperature (20 °C ±2). A DC power supply powers the Peltier module. The sample, Peltier module, and heat sink are tightened with a manual mechanical loading system while a load is monitored using a 2 kN load cell placed on the bottom, as shown in Figure 4.

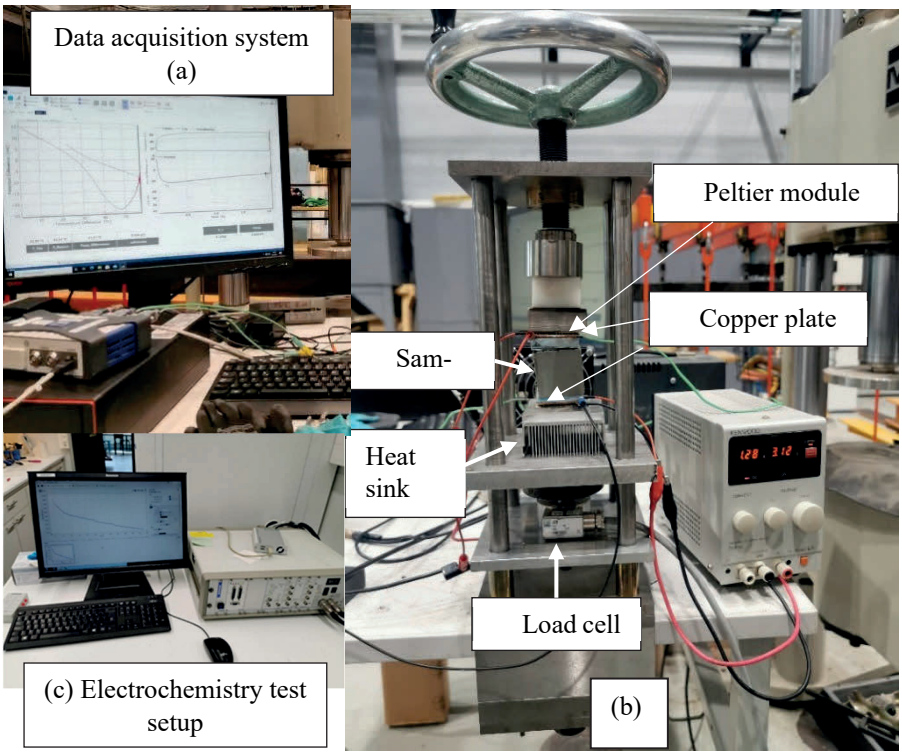

Figure 4. Thermoelectric test setup (a) Data acquisition system, (b) loading setup and (c) Electrochemistry test setup

The measurements are collected using the HBM data acquisition system and controlled using CatmanEasy AP commercial software, where data recording is set to 10 readings per second. The potential difference, upper and lower temperature, and applied load are recorded along with time. Measurements are only started after monitoring the development of potential difference over time to ensure stability of the results.

Electrochemical measurements are carried out using Autolab potentiostat PSTAT100 to determine the ionic conductivity of the samples. Electrochemical measurements are performed in a two-electrode system. Electrochemical impedance spectroscopy (EIS) measurements are conducted at a 2500 to 0.05 Hz frequency range. First, 50 mV voltage amplitude at open circuit potential (OCP) is applied to excite the working electrode. EIS measurements are first recorded at room temperature. Then the power supply is turned on to heat the Peltier modules, where the thermoelectric data is recorded as discussed in section 2.4.1. It should be noted that wire leads connected to the sample are switched between the two measurements to avoid misleading data. Then, the EIS data are recorded when the module reaches a constant temperature.

2.5. Results and Discussion

2.5.1. Material characterization

SEM characterization shows the purity of the MnO_2. Different consecutive photos are taken with different focus of 500µm, 30µm, 4µm and 1µm as shown in Figure 5. The MnO_2 appears to be stacked flakes that form hollow spheres with a diameter of around 5 µm.

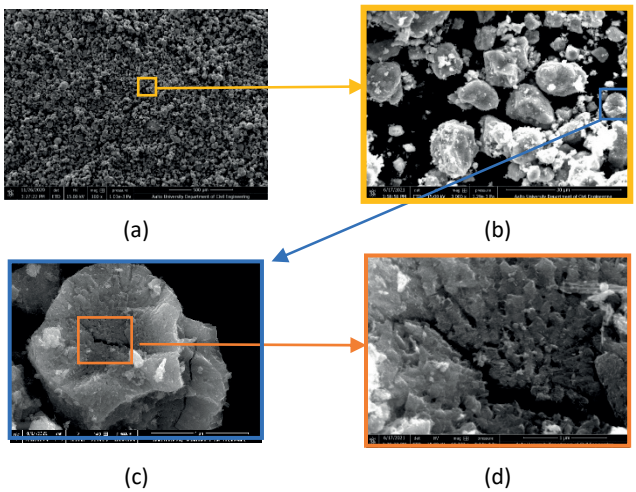

Figure 5. SEM for MnO_2 – (a) 500µm, (b) 30 µm, (c) 4 µm, (d) 1 µm

XRD characterization of the MnO_2 powder shown in Figure 6 exhibits major diffraction peaks at 23.88º, 37.21º, 42.57º, 56.5º, 65.25º, and 69.3º, corresponding to the (116), (419), (218), (297), (45) and (53), (600) diffraction, respectively. In addition, the result aligns entirely with the peaks of ε -MnO_2 reference (ICPDS No. 00-030-0820), confirming the crystal phase of the sample[9].

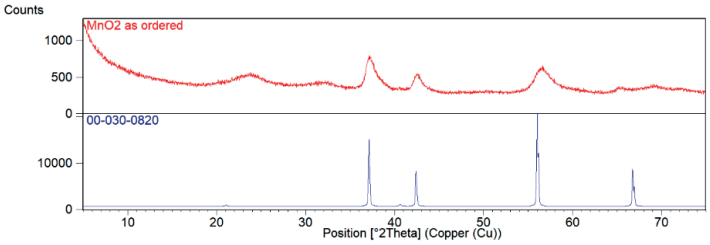

Figure 6. XRD analysis for MnO_2 in reference to ε-MnO_2 (ICPDS No. 00-030-0820)

2.5.2. Evaluation of thermoelectric power for MnO_2 powder

MnO_2 powder is tested to evaluate the thermoelectric power. Figure 7 shows that the Seebeck coefficient ranges from -253 µV/°C to -267 µV/°C for temperatures from -14 °C to 60 °C. A figure of merit ZT of MnO_2 reached 1.289×10^{-6} and is calculated using:

$$ZT = \frac{\sigma S^2 T}{\kappa}$$

where S is the Seebeck coefficient, σ is the electrical conductivity, κ is the thermal conductivity, and T is temperature.

For validation purposes, the MnO_2 powder is tested using the test setup discussed in 2.4.1. Figure 8 shows the potential difference versus temperature difference. Seebeck coefficient can be calculated as the slope of the curve yielding -268.7 µV/°C, which shows a good agreement between the two evaluation techniques and validate the in-house thermoelectric test setup.

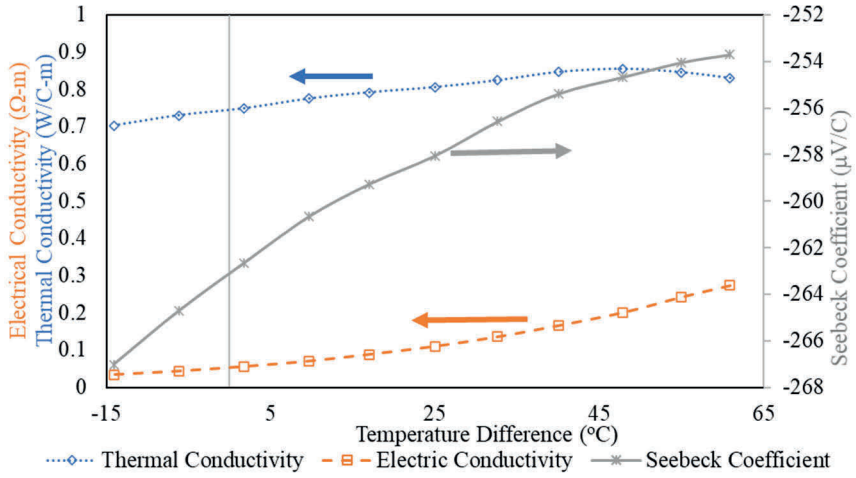

Figure 7. Seebeck Coefficient, Electrical conductivity, and thermal conductivity measured using PPMS® DynaCool™ system

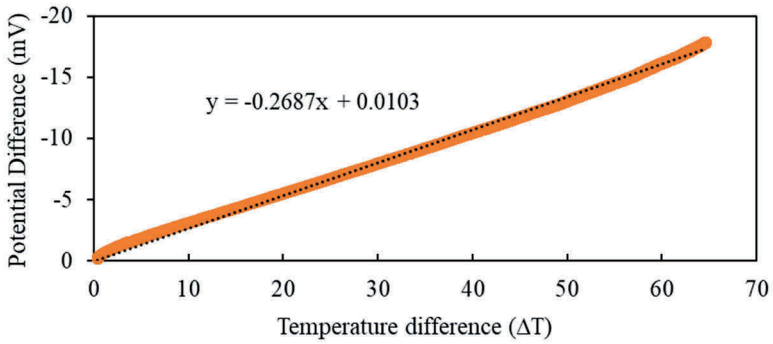

Figure 8. Potential difference vs. temperature difference using an in-house test setup

Typical thermoelectric measurements are shown in Figure 9. The figure shows four stages, starting with (a) heating and electronic thermoelectric generation and (b) ionic thermoelectric generation. Then, upon turning off the power supply, the sample starts to cool down, showing (c) electronic thermoelectric cooling mechanism, then (d) stabilization of ions. Seebeck is measured using the potential and temperature difference

in stage (a) and stage (c). It can be noted that in a dry state, Figure 9 turns from a parallelogram to a line, as shown in Figure 8, where there is no ionic conductivity to generate electricity from ions.

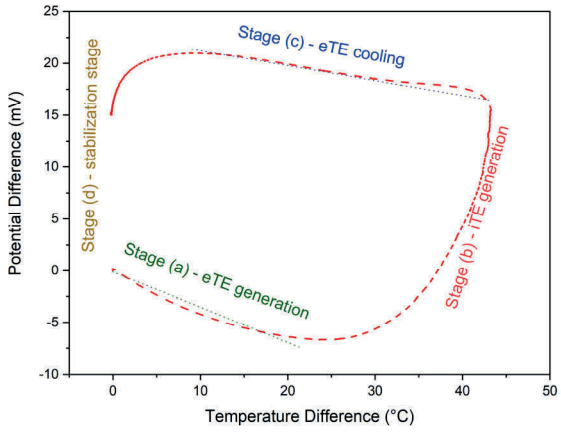

Figure 9. Typical Potential -Temperature difference cycle showing the four stages

EIS is used to investigate the effect of temperature, KOH concentration, and MnO_2 on the ionic performance. The experimental results show the same behavior with varying resistance and capacitance values. The experimental results are then fitted by the equivalent circuit model shown in Figure 10 to obtain the ionic conductivity and capacitance values. The Rb is the bulk resistance and can be correlated to the electrical conductivity of the samples. The value for the R1 element is obtained from the diameter of the semicircle in Nyquist plots. This element is inversely proportional to the ionic conductivity. CPE-1 and CPE-2 elements are proportional to the capacity of the active materials and diffusion coefficient of the ions in the bulk electrolyte, respectively.

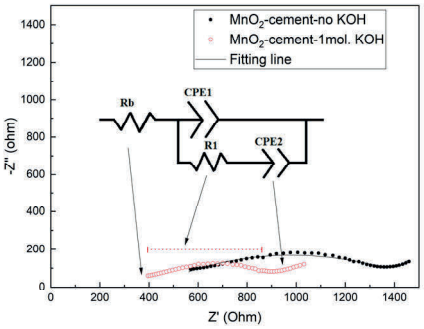

Figure 10. Nyquist plots showing the effect of KOH (samples S1 and S2)

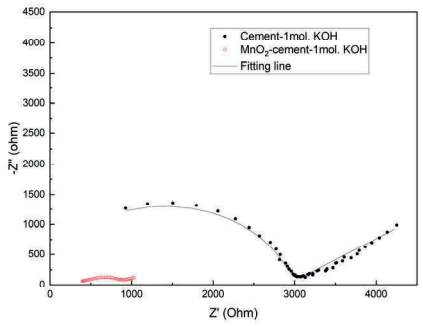

Figure 11. Nyquist plots showing the effect of MnO_2 (samples S3 and S2)

The sample without KOH (S1) is compared to sample with 1mol. KOH (S2) is shown in Figure 10. The effect of KOH is shown in Table 4. The addition of 1 mol. KOH in

sample S2 has slightly enhanced the Seebeck coefficient from -365 to -391 µV/°C while increasing the ionic conductivity by 37%.

Cement paste samples are compared with and without MnO_2 in terms of the Seebeck coefficient. The effect of adding the MnO_2 shown in Table 4 and Figure 11 shows that the core sample without MnO_2 (S3) has limited ionic conductivity compared to the sample S2 which include MnO_2. Therefore, MnO_2 in the core sample works as an electrode material in addition to its thermoelectric capabilities.

Table 4. Effect of KOH concentration and MnO_2

Samples	S (µV/°C)	Ionic Conductivity (S.cm^{-1})
S1-MnO_2-cement	-365,34	0,002643
S2-MnO_2-cement-1mol. KOH	-391,37	0,004227
S3-Cement-1m KOH	43	0,000987

The heat effect is studied on all the samples in terms of ionic conductivity. In all samples, the high temperature increases ionic conductivity. The increase in ionic conductivity ranged from 7% to 18% as shown in Figure 12. Therefore, a higher temperature gradient enhances the overall ionic thermoelectric generation.

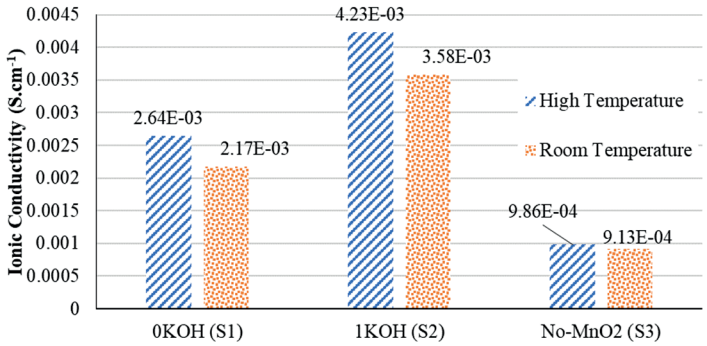

Figure 12. Effect of temperature for all samples in terms of ionic conductivity

2.5.2.1. Effect of inner core size on strength

Extra samples are manufactured to investigate the effect of inner core size on the overall strength of the sample. First, inner cores of different sizes are using diameters of 8 mm, 10 mm, and 12 mm, in addition to the 10x20 mm rectangular shape used in all reported measurements. Then, samples are fabricated following the same procedure discussed in the section 2.2.1, including casting the outer shell of UHSC. After curing for 28 days, samples are tested under compression loading with preloading of 15 MPa using universal machine of Toni Technik with a test speed of 0.6 MPa/sec. Samples are tested placing the samples horizontally to simulate the position of the core inside a vertical building façade. Results in Figure 13 show that the cubes with a diameter of 8

mm are of the same strength as the solid cube. However, the increase of the inner core diameter to 10 mm, 12 mm, and 10x20 mm drop the strength by around 16%, 37%, and 45%, respectively. While there is a significant drop of 45% of strength compared to a solid 40x40x40 mm UHSC cube strength, the strength of the cube with 10x20 mm inner core is still higher than cement paste samples or cement paste with additional powder, which break at a compressive strength of 2 MPa on average. This study indicates that the inner core size, scale dependence of concrete material and its natural variation are factors that need to be considered while designing a load bearing member.

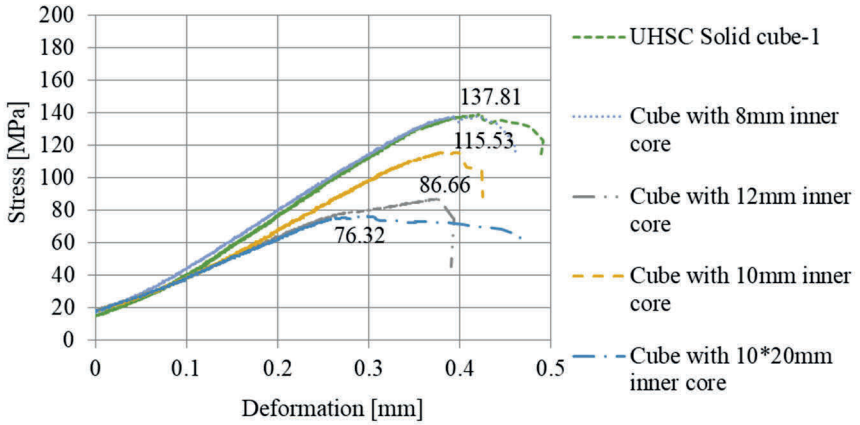

Figure 13. Effect of inner core size on the overall strength

3. Conclusions

A thermoelectric concrete generator is developed using MnO_2 nanopowder. Integrating the MnO_2 nanopowder material with the cement paste is essential to produce thermoelectric power and store charge. A novel way is presented to generate the thermoelectric performance while enhancing the strength through casting UHSC around the sample. Samples are tested under normal conditions, i.e., moisture content within samples is kept without drying. A study is carried out to investigate the effects of KOH, MnO_2, high-temperature gradient on the ionic conductivity, and the effect of inner core size on the overall strength. It can be concluded that:

1. The addition of MnO_2 powder contributed to both ionic and electronic thermoelectric generation. Conversely, samples without MnO_2 have a very low Seebeck coefficient.
2. KOH enhanced the Seebeck coefficient and ionic conductivity.
3. Innovative integration of the inner core MnO_2-cement-1KOH within UHSC results in a Seebeck coefficient of -391μV/°C while having a strength of 76,3 MPa.
4. The compressive strength tests of the UHSC member indicate that the inner core size, scale dependence of concrete material and its natural variation are

factors to be considered in designing a load bearing member of thermoelectric concrete.

Future research is needed to study the effect of the inner core size on the ionic conductivity and power generation of combined n and p-type ionic and electronic thermoelectric.

Acknowledgment

The authors would like to thank the civil engineering laboratory staff. In addition, the authors would like to thank Ramzy Abdelaziz and Ville Liljeström from NanoMicroscopy Center (NMC) for using the SEM and XRD equipment. The funding from Academy of Finland Postdoctoral fellowship (348611) and Auramo-säätiö is highly appreciated.

References

[1] S. Wen and D. D. L. Chung, "Seebeck effect in carbon fiber-reinforced cement," *Cem. Concr. Res.*, vol. 29, no. 12, pp. 1989–1993, 1999, doi: 10.1016/S0008-8846(99)00185-4.

[2] S. Wen and D. D. L. Chung, "Seebeck effect in steel fiber reinforced cement," *Cem. Concr. Res.*, vol. 30, no. 4, pp. 661–664, 2000, doi: 10.1016/S0008-8846(00)00205-2.

[3] L. Tzounis, M. Liebscher, R. Fuge, A. Leonhardt, and V. Mechtcherine, "P- and n-type thermoelectric cement composites with CVD grown p- and n-doped carbon nanotubes: Demonstration of a structural thermoelectric generator," *Energy Build.*, vol. 191, pp. 151–163, 2019, doi: 10.1016/j.enbuild.2019.03.027.

[4] J. Wei, L. Hao, G. He, and C. Yang, "Enhanced thermoelectric effect of carbon fiber reinforced cement composites by metallic oxide/cement interface," *Ceram. Int.*, vol. 40, no. 6, pp. 8261–8263, 2014, doi: 10.1016/j.ceramint.2014.01.024.

[5] S. Ghosh, S. Harish, K. A. Rocky, M. Ohtaki, and B. B. Saha, "Graphene enhanced thermoelectric properties of cement based composites for building energy harvesting," *Energy Build.*, vol. 202, pp. 1–7, 2019, doi: 10.1016/j.enbuild.2019.109419.

[6] T. Ji, X. Zhang, and W. Li, "Enhanced thermoelectric effect of cement composite by addition of metallic oxide nanopowders for energy harvesting in buildings," *Constr. Build. Mater.*, vol. 115, pp. 576–581, 2016, doi: 10.1016/j.conbuildmat.2016.04.035.

[7] T. Ji, X. Zhang, X. Zhang, Y. Zhang, and W. Li, "Effect of manganese dioxide nanorods on the thermoelectric properties of cement composites," *J. Mater. Civ. Eng.*, vol. 30, no. 9, pp. 1–8, 2018, doi: 10.1061/(ASCE) MT.1943-5533.0002401.

[8] J. Wei *et al.*, "Record high thermoelectric performance of expanded graphite/carbon fiber cement composites enhanced by ionic liquid 1-butyl-3-methylimidazolium bromide for building energy harvesting," *J. Mater. Chem. C*, pp. 3682–3691, 2021, doi: 10.1039/d0tc05595f.

[9] A. J. Roberts and R. C. T. Slade, "Controlled synthesis of ε-MnO2 and its application in hybrid supercapacitor devices," *J. Mater. Chem.*, vol. 20, no. 16, pp. 3221–3226, 2010, doi: 10.1039/b924247c.